UDK 620.1:537.8:621.793.8:621.3.014.31
Original scientific article/Izvirni znanstveni članek

ISSN 1580-2949
MTAEC9, 53(6)833(2019)

EFFECT OF AN ELECTROMAGNETIC FIELD ON THE MICROSTRUCTURE AND PROPERTIES OF Cr(Ti)AlN HARD COATINGS PREPARED WITH ARC-ION PLATING

VPLIV ELEKTROMAGNETNIH POLJ NA MIKROSTRUKTURO IN LASTNOSTI TRDIH PREVLEK NA OSNOVI Cr(Ti)AlN, PRIPRAVLJENIH S PLATIRANJEM V IONSKEM OBLOKU

Jin Wang[1]*, Dayan Ma[2], Qi Liu[2], Yetang Jin[1], Xu Wang[1]

[1]School of Mechanical Engineering, Qingdao University of Technology, Qingdao 266520, China
[2]State Key Laboratory for Mechanical Behavior of Materials, Xi'an Jiaotong University, Xi'an 710049, China

Prejem rokopisa – received: 2019-04-03; sprejem za objavo – accepted for publication: 2019-06-27

doi:10.17222/mit.2019.072

A series of CrAlN and TiAlN hard coatings were prepared using industrial arc-ion plating with or without the embedded axial electromagnetic filtration technology. The microstructure evolution and mechanical properties of the hard coatings were compared after annealing. The results show that the grain size of the hard coatings prepared with an arc induced by an electromagnetic field decreases significantly, and the quantity of pits and hard particles reduces, leading to an improvement of compactness. Furthermore, the wear resistance and the thermal stability of the coatings prepared with electromagnetic fields improve significantly.

Keywords: arc-ion plating, axial electromagnetic field, microstructure evolution, mechanical property, wear resistance

Avtorji so pripravili vrsto CrAlN in TiAlN trdih prevlek na industrijski napravi za ionsko obločno platiranje, brez ali v prisotnosti osne elektromagnetne filtracijske tehnologije. Nato so med seboj primerjali razvoj mikrostruktur in mehanske lastnosti izdelanih trdih prevlek po njihovem naknadnem žarjenju. Rezultati raziskave so pokazali, da se je velikost kristalnih zrn trdih prevlek, izdelanih v prisotnosti elektromagnetnih polj, pomembno zmanjšala. Zmanjšala se je tudi količina jamic in trdih delcev, kar je izboljšalo kompaktnost trdih prevlek. Poleg tega se je znatno izboljšala tudi odpornost proti obrabi in termična stabilnost prevlek, izdelanih v elektromagnetnih poljih.

Ključne besede: platiranje v obloku ionov, osno elektromagnetno polje, razvoj mikrostrukture, mehanske lastnosti, odpornost proti obrabi

1 INTRODUCTION

Arc-ion plating is a deposition process with a high ion energy and high speed, suitable for many kinds of materials, and a simple cleaning process before preparation.[1–4] The deposition technology is widely used in the industrial surface engineering of hot-working dies. However, it is known that the inevitable appearance of hard particulates in the process of preparation have negative influences on the application effectiveness of the coating dies.

Recently, the arched electromagnetic field was developed in order to reduce the size and number of hard particles in coatings. TiN coatings have been deposited by adding an arched electromagnetic field on the cathode arc source, and the mechanical properties of the coatings have been greatly improved.[5,6] However, the ion-deposition rate of the arched electromagnetic field is too slow to be applied in industry. In order to handle the problem of the low deposition rate, the axial electromagnetic field was developed. The extra-axial magnetic field can make the arc spot move at a high speed, steadily and regularly within circular and radial shrinkage.[7,8] As the temperature of the target surface decreases, restricting the growth of grains, the grain size decreases. Simultaneously, the size of hard particulates decreases, resulting in an improvement of the compactness of the coatings. Q. Zhang[9,10] prepared AlTiN coatings using a cathode arc-source device with an axial magnetic field. The hardness of the coatings increased significantly.

At present, the design and analysis of electromagnetic fields are receiving a lot of attention. However, there is still little research on the effect of electromagnetic fields on the comprehensive properties of coatings. In this study, a series of ternary coatings were synthesized using traditional arc-ion plating with an axial electromagnetic field. The corresponding mechanical, tribological and high-temperature oxidation-resistance properties were characterized.

*Corresponding author's e-mail:
wangjin@qut.edu.cn (Jin Wang)

Table 1: Processes and parameters for the four kinds of coatings

	Pressure (Pa)	Tempera-ture (°C)	Time (min)	Bias (V)	Target current (A)			Gas (sccm)		Electromagnetic voltage (V)
					Cr	CrAl	TiAl	N_2	Ar	
Glowing	0.3	450	40	800	–	–	–	–	20	–
Cr bombardment	0.3	450	30	200	110	–	–	–	20	–
CrN	1.5	450	15	110	110	–	–	240	15	–
1-CrAlN	3.0	450	–	70	–	70	–	350	0	–
2-TiAlN	3.0	450	–	70	–	–	70	350	0	–
3-CrAlN(EM)	3.0	450	–	70	–	70	–	350	0	15
4-TiAlN(EM)	3.0	450	–	70	–	–	70	350	0	15

2 EXPERIMENTAL PART

2.1 Preparation of ternary composite coatings

The coatings were deposited on samples of H13 steel using the industrial technology of arc ion plating with a magnetic filter ring for generating an axial electromagnetic field, as shown in **Figure 1**. The samples were polished on a metallographic grinding machine, and then placed in an anhydrous ethanol solution for ultrasonic cleaning for 20 min. After the cleaning, the samples were placed into a vacuum chamber with a background pressure of 3×10^{-4} Pa for the deposition of coatings. The deposition process was followed by glowing, Cr bombardment, deposition of the bottom layer and deposition of the functional layer. Specific parameters of each step are shown in **Table 1**. A 99.9 % pure Cr target, a $Cr_{0.33}Al_{0.67}$ target and four $Ti_{0.33}Al_{0.67}$ targets, which were circular thin targets with a diameter of 100 mm and a thickness of 15 mm, were employed. To distinguish whether the electromagnetic fields were used in the preparation of hard coatings, formulas CrAlN(EM) and TiAlN(EM) were used to indicate that they were prepared with electromagnetic fields while CrAlN and TiAlN indicate that they were prepared without electromagnetic fields.

2.2 Test methods

The deposited samples were annealed at 700 °C in a programmable protective-atmosphere box furnace for 30 min. The thickness and hardness of the coatings were measured with a ball marker (JS-QHY-2) and a micro-Vickers hardness tester (HXD-1000TM / LCD). The anti-crack critical load Lc1 and failure load Lc2 of the coatings were measured with a scratch tester (WS-2005) for the quantitative adhesion analysis. The friction coefficients on the surfaces of the coatings were measured with a UMT multi-purpose friction-and-wear testing machine to analyze the wear resistance. The surface morphologies and microstructures of the coatings were analyzed with a scanning electron microscope (SEM) (ZEISS MERLIN COMPACT) and Nordlys Max EDS. The phase structures of the coatings were analyzed with X-ray diffraction (XRD) (Rigaku D/max-2550/PC). The grain sizes of the coatings were calculated with the Scherrer formula.

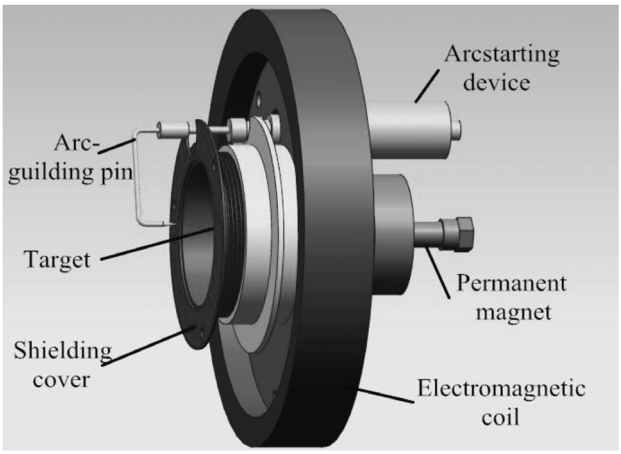

Figure 1: Schematic diagram of the electromagnetic arc source

3 RESULTS AND DISCUSSION

3.1 Microstructure of coatings

The XRD pattern of each coating after annealing in air is shown in **Figure 2**. The main structure of each coating is a NaCl-type face-centered-cubic structure (FCC). The CrAlN and CrAlN(EM) coatings mainly consist of the fcc-Cr(Al)N phase with preferred (200) orientation. The TiAlN and TiAlN (EM) coatings mainly consist of the fcc-Ti(Al)N phase, also showing a preferred orientation of the crystal plane (200). In addition,

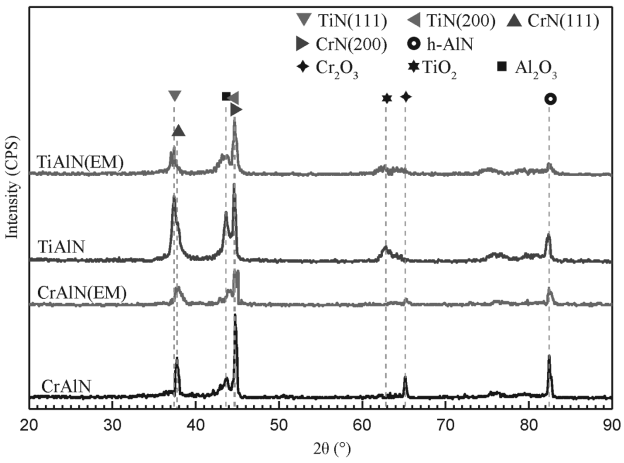

Figure 2: XRD patterns for the coatings annealed in air

the metastable h-AlN phase appears in all the coatings. The h-AlN diffraction-peak intensity of the CrAlN and TiAlN coatings increases gradually, but the (111) and (200) plane diffraction-peak intensity of the CrN and TiN phase decreases compared with that of the CrAlN(EM) and TiAlN(EM) coatings. This suggests that the nucleation energy of h-AlN was reduced and the growth of the (111) and (200) planes was promoted by the addition of the axial electromagnetic field. It was shown that when the amount of Al is high (50–77 %) and the temperature is high, the energy required for the Al atoms to be embedded in the lattice is higher than that for the H-AlN nucleation, and the H-AlN phase is easily formed.[11–13] In this study, the EDS analysis of various coatings indicates that the Al amount is above 50 %, which is in agreement with the results of the reference studies (**Figure 3**).

The grain size was calculated with the Scherrer formula. The grain sizes of the CrAlN (EM) and TiAlN (EM) coatings are 14.8 nm and 15.2 nm, respectively. In comparison, the grain sizes of the CrAlN and TiAlN coatings are 16.8 nm and 17.9 nm, respectively. The results imply that the grain size can be refined with an axial electromagnetic field. When the electromagnetic voltage increases within a certain range, the arc-spot movement accelerates, the target ionization rate increases, the density and energy of plasma improve relatively. The ion-bombardment energy increases with the acceleration of the substrate bias voltage, which leads to more defects on the coating surface,[14] resulting in an increase of the preferential nucleation sites and a decrease of the grain size.

The oxidation resistance of various coatings was also analyzed with XRD as shown in **Figure 2**. The diffraction peaks of Al_2O_3 and Cr_2O_3 mainly appear for the CrAlN and CrAlN(EM) coatings. The diffraction peaks of Al_2O_3 and TiO_2 are mainly in the TiAlN and TiAlN(EM) coatings. In contrast, the order of oxidation diffraction peaks from high to low is as follows: TiAlN, CrAlN, TiAlN(EM) and CrAlN(EM). This is due to the mixed oxides of Al_2O_3 and Cr_2O_3, which are formed on the surfaces of the coatings, and are more compact than the structures of the CrAlN and CrAlN(EM) coatings. They can be an effective barrier to the oxygen diffusion into the interior at a high temperature, increasing the oxidation resistance of the coatings.[15,16] However, the mixed oxides in the TiAlN and TiAlN (EM) coatings are Al_2O_3 and TiO_2. TiO_2 is a columnar structure with voids around it, resulting in a decrease in the oxidation resistance of the coatings.[17]

As shown in **Figure 4**, the surface morphology of the coatings was analyzed with SEM, and it was found that there are more pits and hard particles on the surfaces of the CrAlN and TiAlN coatings than on the surfaces of the CrAlN(EM) and TiAlN(EM) coatings (**Figures 4a** to **4ff**). After the annealing at 700 °C, the oxidation around the pits and hard particulates on the surfaces of the CrAlN and TiAlN coatings, and the size and number of hard particulates increase (**Figure 4c and 4g**). However, the surface morphology of the CrAlN(EM) and TiAlN(EM) coatings shows no change after high-tem-

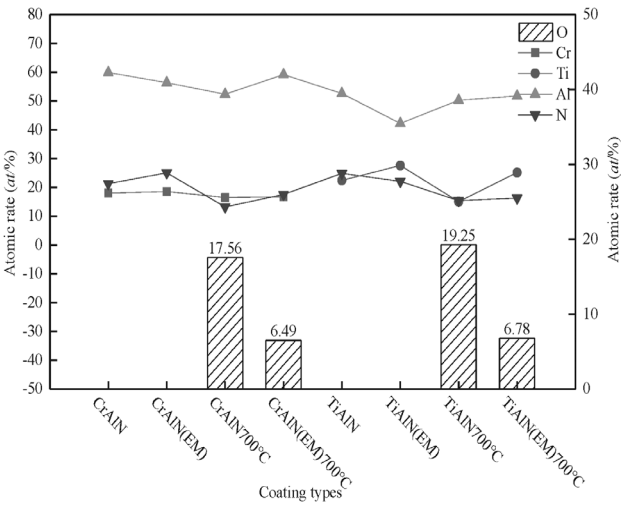

Figure 3: Element amounts in the four coatings before and after the annealing

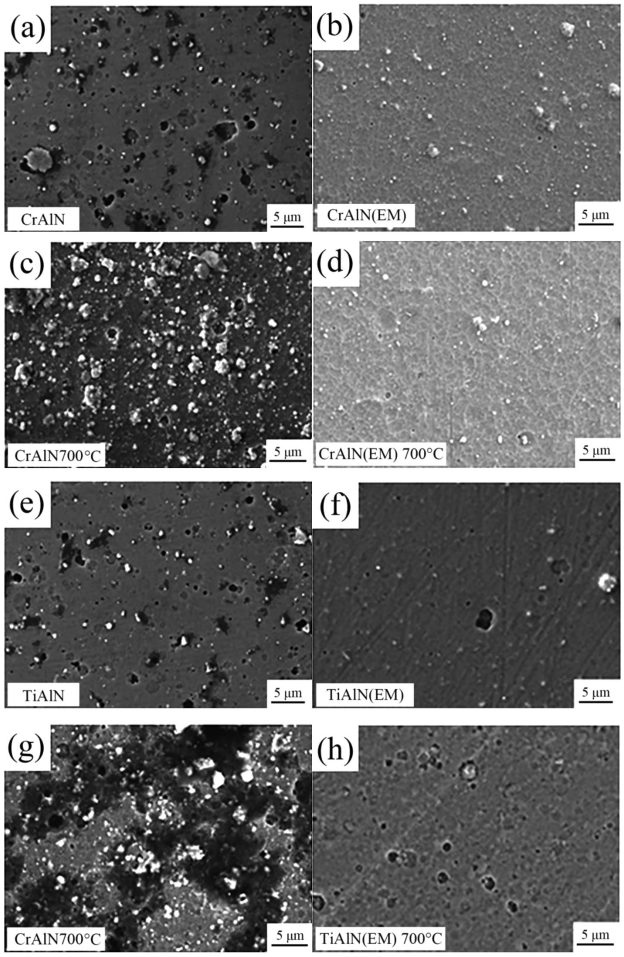

Figure 4: SEM images of TiAlN and CrAlN coatings before and after annealing

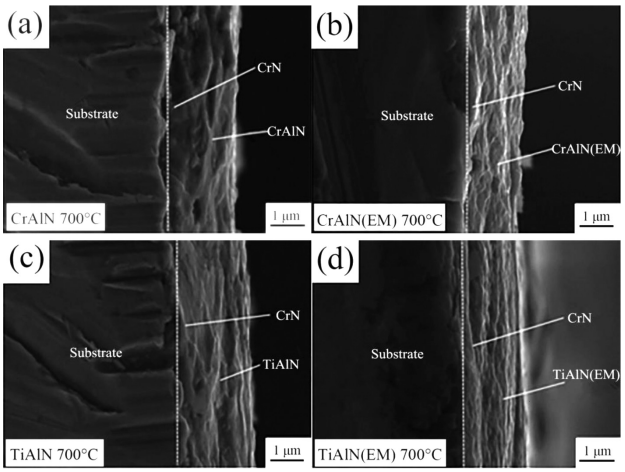

Figure 5: Cross-sectional SEM images of different coatings annealed in air at 700 °C for 30 min

perature annealing (**Figure 4d, 4h**). Furthermore, the EDS analysis of the O element (**Figure 3**) shows that the atomic percentage of O in the CrAlN, TiAlN, CrAlN(EM) and CrAlN(EM) coatings is 17.56, 17.56, 6.49 and 6.78 %, respectively. The results are in agreement with those of the surface morphology and XRD. The results also show that CrAlN(EM) and CrAlN(EM) have better oxidation resistance than CrAlN and TiAlN.

Figure 5 shows the SEM cross-sectional morphology of the coating elements after the annealing. It is observed that the internal structure of the coatings is an equiaxed nanocrystalline rather than the traditional columnar structure. The reason is that the columnar epitaxial growth of the grains was limited by adjusting the bias voltage, electromagnetic coil voltage, target current and vacuum in the process of the coating preparation.[18,19] Furthermore, no obvious oxide layers are observed in the cross-sectional morphologies of the coatings, indicating that the oxidation reaction occurred only in the local regions of the coating surfaces, and the coatings did not fail completely.

3.2 Tribological properties

The wear-scar morphologies and the average friction coefficients of the coatings before and after the annealing are shown in **Figures 6** and **7**. Before the annealing, the friction coefficients of the CrAlN and TiAlN coatings are relatively high, and there are many pits in the wear scar; the wear mechanism is mainly adhesive wear. However, the number and size of the pits on the surfaces of the wear scars of the CrAlN(EM) and TiAlN(EM) coatings significantly decrease and the friction coefficients decrease. After the annealing, although the friction coefficients of the CrAlN and TiAlN coatings decrease greatly, they are still higher than those of the CrAlN (EM) and TiAlN (EM) coatings. This can be explained with the fact that the internal structures of the CrAlN and TiAlN coatings are not compact, resulting in the Al

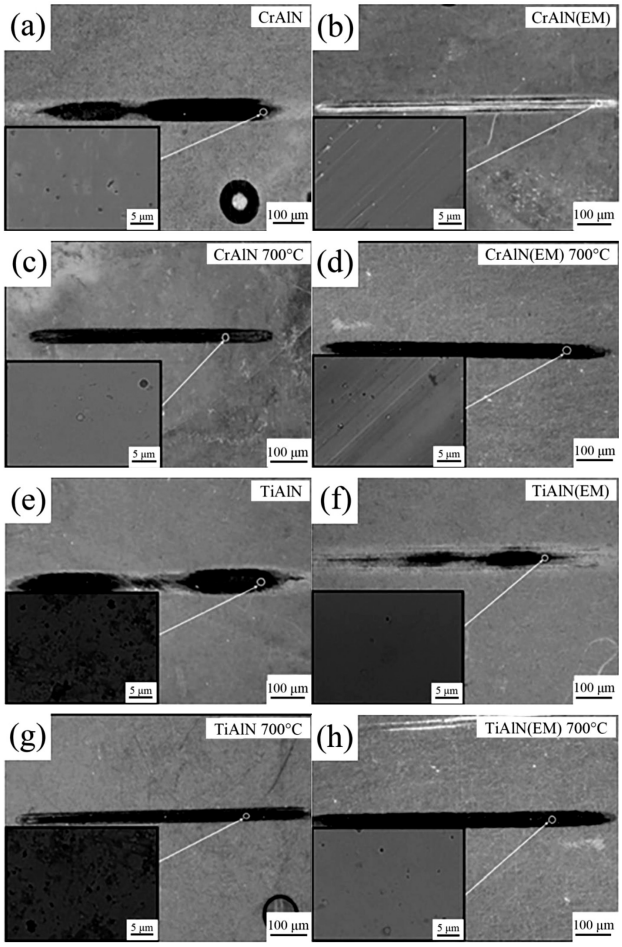

Figure 6: Wear morphologies of coatings before and after annealing

element contacts with the O element to form Al_2O_3 with self-lubricating in the process of annealing, which plays a role of solid lubrication. When in contact with O, the Cr element can form Cr_2O_3 with high hardness and heat resistance, which is beneficial to chip removal.[20,21] The columnar amorphous TiO_2 formed due to the contact of

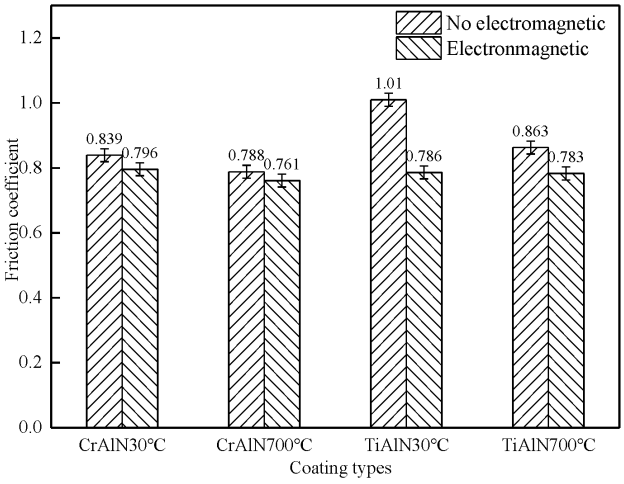

Figure 7: Average friction coefficients of coatings before and after annealing

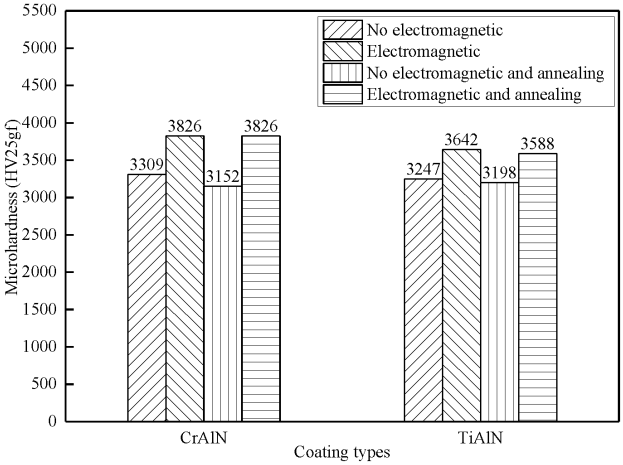

Figure 8: Average microhardness values of deposited and annealed coatings

Ti with O not only has a poor chip-removal ability, but also has voids, leading to continuous oxidation.[22] It is worth noting that the wear mechanism of the CrAlN (EM) coating changes from the adhesive wear to the abrasive wear, not only due to the formation of Al_2O_3, but also due to the changes in the parameters of the electromagnetic filter device.

3.3 Mechanical properties

After the testing, the thickness of the CrAlN, CrAlN(EM) and TiAlN, TiAlN(EM) are (5.32, 5.29, 5.08 and 5.21) μm. **Figure 8** shows the hardness of the coatings before and after the annealing. The microhardness levels of the CrAlN(EM) and TiAlN(EM) coatings are higher than those of the CrAlN and TiAlN, respectively. The improvement of the coating hardness is mainly caused by the Hall-Petch effect merged with the Al solid solution in CrN or TiN, resulting in solid-solution strengthening, fine-grain strengthening and an abundant formation of the ceramic phase with an increase in the N amount.[23,24] In this study, the amounts of Al and N are almost the same according to the EDS analysis, indicating that the improved hardness of the CrAlN(EM) and TiAlN(EM) coatings is due to fine-grain strengthening. The axial magnetic field increases the energy of the deposited ions and enhances the nucleation rate of the grains, resulting in grain refinement. After the annealing, the hardness of the CrAlN(EM) and TiAlN(EM) coatings still remains stable, while the hardness of the CrAlN and TiAlN coatings decreases. This suggests that the addition of the axial electromagnetic field reduces the soft hcp-AlN phase and residual stress of the CrAlN(EM) and TiAlN(EM) coatings.

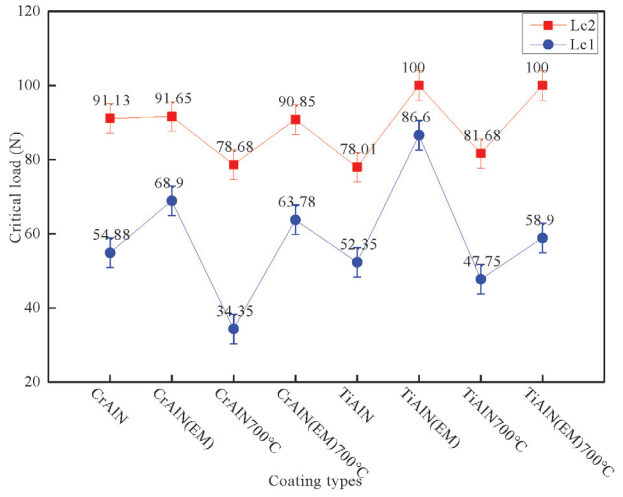

Figure 9: Critical load (Lc1, Lc2) of deposited and annealed coatings

The adhesive force of each coating was quantitatively analyzed with the scratch method. The critical load of the crack resistance (Lc1) and the failure critical load (Lc2) before and after the annealing are shown in **Figure 9**. Critical loads Lc1 and Lc2 of the CrAlN(EM) and TiAlN(EM) coatings with a small grain size, compact structure, and low compressive stress are significantly higher than those of the CrAlN and TiAlN coatings. Lc1 and Lc2 are mainly determined with the residual stress of the coatings, which can cause the coatings to be exfoliated by separating the coating from the substrate and subsequent wrinkling. High-temperature annealing can increase the residual stress of the coatings. Therefore, Lc1 and Lc2 of the CrAlN and TiAlN coatings decrease significantly after annealing. The electromagnetic field increases the compactness of the coatings and reduces the residual stress. Therefore, after annealing, Lc1 and Lc2 of CrAlN(EM) and TiAlN(EM) are significantly higher than those of CrAlN and TiAlN, and the stability of the binding force of CrAlN(EM) and TiAlN(EM) is better.

4 CONCLUSIONS

A series of CrAlN and TiAlN coatings were prepared using arc-ion plating with and without an axial electromagnetic field. The effects of the axial magnetic field on the microstructure and mechanical properties of the two coatings were compared. The main conclusions are as follows:

1) Axial electromagnetic field can significantly refine the grain size of the two coatings and improve their oxidation resistance.

2) Axial electromagnetic field can significantly reduce the pits and hard particles on the surfaces of the two coatings, reducing the friction coefficient and improving the wear resistance.

3) Axial electromagnetic field can increase the hardness of the two coatings and improve the bond between the coatings and the substrate.

4) After annealing, the mechanical properties of the two coatings prepared with the axial electromagnetic field can still be maintained.

Acknowledgment

This work was supported by the Key R & D projects of Shandong Province under Grant No.2019GGX102023 and the National Natural Science Foundation of China under Grant Nos. 51205217 and 51775289.

5 REFERENCES

[1] H. Lille, A. Ryabchikov, E. Adoberg, L. Kurissoo, P. Peetsalu, L. Lind, Evaluation of residual stresses in PVD coatings by means of the curvature method of plate, Key Eng. Mater., 721 (**2016**), 404–408, doi:10.4028/www.scientific.net/kem.721.404

[2] J. Lawal, P. Kiryukhantsev-Korneev, A. Matthews, A. Leyland, Mechanical properties and abrasive wear behaviour of Al-based PVD amorphous/nanostructured coatings, Surf. Coat. Technol., 310 (**2017**), 59–69, doi:10.1016/j.surfcoat.2016.12.031

[3] C. Puneet, K. Valleti, A. V. Gopal, Influence of surface preparation on the tool life of cathodic arc PVD coated twist drills, J. Manuf. Process., 27 (**2017**), 233–240, doi:10.1016/j.jmapro.2017.05.011

[4] M. Yousfi, J. C. Outeiro, C. Nouveau, B. Marcon, B. Zouhair, Tribological behavior of PVD hard coated cutting tools under cryogenic cooling conditions, Procedia CIRP, 58 (**2017**), 561–565, doi:10.1016/j.procir.2017.03.269

[5] M. Amati, L. Gregoratti, H. Sezen, A. Grce, M. Milosavljević, K. P. Homewood, Compositional and structural studies of ion-beam modified AlN/TiN multilayers, Appl. Surf. Sci., 411 (**2017**), 431–436, doi:10.1016/j.apsusc.2017.03.160

[6] X. W. Shi, X. G. Li, W. Q. Qiu, Z. Y. Liu, Hardening mechanism of TiN coating by magnetic filtered arc ion plating, Chin. J. Vac. Sci. Technol., 28 (**2008**), 486–491, doi:10.13922/j.cnki.cjovst.2008.05.013

[7] L. Chen, Z. L. Pei, J. Q. Xiao, J. Gong, C. Sun, TiAlN/Cu nanocomposite coatings deposited by filtered cathodic arc ion plating, J. Mater. Sci. Technol., 33 (**2016**), 111–116, doi:10.1016/j.jmst.2016.07.018

[8] W. C. Lang, J. Q. Xiao, J. Gong, C. Sun, R. F. Huang, L. S. Wen, Study on cathode spot motion and macroparticles reduction in axisymmetric magnetic field-enhanced vacuum arc deposition, Vacuum, 84 (**2010**), 1111–1117, doi:10.1016/j.vacuum.2010.01.037

[9] Q. Zhang, C. Qiu, J. Liang, D. Geng, Q. Wang, Influence of electromagnetic field on properties of arc-ion plated AlTiN coatings, Chin. J. Vac. Sci. Technol., 36 (**2016**), 666–671, doi:10.13922/j.cnki.cjovst.2016.06.11

[10] W. Lang, Y. Zhao, J. Xiao, J. Gong, C. Sun, B. Yu, L. Wen, Influence of rotating transverse magnetic field on motion of cathode spot in arc ion plating, Chin. J. Vac. Sci. Technol., 35 (**2015**), 316–322, doi:10.13922/j.cnki.cjovst.2015.03.12

[11] P. H. Mayrhofer, H. Willmann, A. E. Reiter, Structure and phase evolution of Cr-Al-N coatings during annealing, Surf. Coat. Technol., 202 (**2008**), 4935–4938, doi:10.1016/j.surfcoat.2008.04.075

[12] Y. Chen, H. Du, M. Chen, J. Yang, J. Xiong, H. B. Zhao, Structure and wear behavior of AlCrSiN-based coatings, Appl. Surf. Sci., 370 (**2016**), 176–183, doi:10.1016/j.apsusc.2015.12.027

[13] W. L. Chen, J. Zheng, Y. Lin, S. Kwon, S. H. Zhang, Comparison of AlCrN and AlCrTiSiN coatings deposited on the surface of plasma nitrocarburized high carbon steels, Appl. Surf. Sci., 332 (**2015**), 525–532, doi:10.1016/j.apsusc.2015.01.212

[14] I. I. Beilis, Vacuum arc cathode spot grouping and motion in magnetic fields, IEEE T. Plasma, 30 (**2002**), 2124–2132, doi:10.1109/tps.2002.807330

[15] C. Sabitzer, J. Paulitsch, S. Kolozsvári, R. Rachbauer, P. H. Mayrhofer, Impact of bias potential and layer arrangement on thermal stability of arc evaporated Al-Cr-N coatings, Thin Solid Films, 610 (**2016**), 26–34, doi:10.1016/j.tsf.2016.05.011

[16] Y. Q. Wei, X. B. Tian, C. Z. Gong, S. Q. Yang, Microstructure and mechanical properties of TiN/TiAlN multilayer coatings deposited by arc ion plating with separate targets, Chin. J. Mater. Res., 25 (**2011**), 630–636, doi:10.1016/s1003-6326(11)60823-6

[17] Y. Xu, Q. Miao, W. P. Liang, L. Wang, X. S. Yu, B. L. Ren, Z. J. Yao, A comparison of oxidation behavior of Al coatings prepared by magnetron sputtering and arc ion plating on y -TiAl, Rare Metal. Mat. Eng., 43 (**2014**), 2652–2656, doi:0.1016/S1875-5372(15)60020-0

[18] M. Zhang, G. Q. Lin, G. Y. Lu, C. Dong, K. H. Kim, High-temperature oxidation resistant (Cr,Al)N films synthesized using pulsed bias arc ion plating, Appl. Surf. Sci., 254 (**2008**), 7149–7154, doi:10.1016/j.apsusc.2008.05.293.

[19] H. Wu, X. H. Li, M. Y. Guo, S. You, Thermal stability of physical vapor deposited (Ti,Al)N hard coating, Chin. J. Vac. Sci. Technol., 36 (**2016**), 130–135, doi:10.13922/j.cnki.cjovst.2016.02.02

[20] H. Willmann, P. H. Mayrhofer, P. O. Å. Persson, A. E. Reiter, L. Hultman, C. Mitterer, Thermal stability of Al-Cr-N hard coatings, Scripta Mater., 54 (**2006**), 1847–1851, doi:10.1016/j.scriptamat.2006.02.023

[21] J. Zhang, W. Tang, C. Mao, K. Tang, X. F. Yu, Phase structure stability and thermal decomposition mechanism of CrAlN hard cutting tool coating, Chin. J. Nonferrous. Met., 26 (**2016**), 88–95, doi:10.19476/j.ysxb.1004.0609.2016.01.011

[22] C. Mastail, M. David, F. Nita, A. Michel, G. Abadias, Ti, Al and N adatom adsorption and diffusion on rocksalt cubic AlN (001) and (011) surfaces: Ab initio calculations, Appl. Surf. Sci., 423 (**2017**), 354–364, doi:10.1016/j.apsusc.2017.06.179

[23] Z. W. Xie, L. P. Wang, X. F. Wang, L. Huang, Y. Lu, J. C. Yan, Microstructure and tribological properties of diamond-like carbon and TiAlSiCN nanocomposite coatings, Surf. Coat. Technol., 206 (**2011**), 1293–1298, doi:10.1016/j.surfcoat.2011.08.047

[24] V. V. Uglov, V. M. Anishchik, S. V. Zlotski, G. Abadias, S. N. Dub, Structural and mechanical stability upon annealing of arc-deposited Ti-Zr-N coatings, Surf. Coat. Technol., 202 (**2008**), 2394–2398, doi:10.1016/j.surfcoat.2007.09.035